7.2

Satellite-Derived Products to Enhance Aviation Nowcasting of Convection, Turbulence, and Volcanic Ash

Wayne F. Feltz*, Kristopher Bedka*, Anthony J. Wimmers*, Michael Pavolonis*, Sarah M. Bedka*, Steve Ackerman*, John R. Mecikalski[#], John J. Murray[+], David B. Johnson[-]

*Space Science and Engineering Center University of Wisconsin – Madison, Madison, Wisconsin

[#]Department of Atmospheric Sciences, University of Alabama, Huntsville, Alabama

[+]Langley Research Center, Atmospheric Sciences Division, Hampton, Virginia

[-]Research Applications Program NCAR P.O. Box 3000 Boulder, CO 80307

1. INTRODUCTION

A NASA LaRC effort, the Advanced Satellite Aviation-weather Products (ASAP) initiative, has been developed to provide satellite-derived meteorological products and expertise to the Federal Aviation Administration (FAA) weather research community. The University of Wisconsin-Madison SSEC/CIMSS, in conjunction with the University of Alabama in Huntsville, MIT, and NCAR/RAP has been tasked to provide satellite-derived information to the NCAR-based Aviation Weather Research Program's (AWRP) Product Development Teams (PDT). Satellite-derived products that ASAP will develop and provide to the AWRP PDTs are value-added information for forecasting/nowcasting aviation hazards such as those caused by low ceiling/visibility, convection, turbulence, icing, volcanic ash, and wind shear. Much of the satellite data provided to NCAR will be infused into each PDT's unique system for diagnosing a particular hazard. For ASAP in 2004 and beyond, UW will collaborate with the University of Alabama in Huntsville (see collaborating poster at conference). This collaboration will bolster UW-Madison ASAP activities by offering expertise in data mining, pattern recognition, as well as through introduction of other remote sensing data sets (e.g., lightning). Phase 2 of ASAP activities will include incorporation of hyperspectral satellite data (AIRS, CrIS, and HES) products into the FAA PDT's aviation hazard algorithms. This paper will present an overview of current University of Wisconsin-SSEC/CIMSS ASAP research and products.

2. SATELLITE CLOUD PRODUCTS

One primary focus of the ASAP initiative is the development and distribution of satellite-derived cloud products to the AWRP PDT's. Currently, cloud amount, cloud top temperature, and cloud-top pressure are available from CIMSS hourly over the CONtinental United States (CONUS). These are derived using geostationary data from the Geostationary Operational Environmental Satellite (GOES)-10 (Western United States) and -12 (Eastern United States) Imager and Sounder instruments. Both the 10 km spatial resolution Sounder and the 4 km spatial resolution Imager products are derived using a multi-spectral approach, utilizing the specific spectral information provided by each instrument. An example of the GOES-12 Imager derived cloud-top height product is shown in Figure 1. Cloud-top height for the GOES-10/12 Sounder, as well as the GOES-12 Imager is derived using a combination of the IR window (Schriener *et al.,* 2001) and CO_2 absorption (Wylie and Menzel, 1989) techniques. The IR window technique is reliable for low and mid-level clouds, while the CO_2 ratio technique offers improvements in height assignment for high, semi-transparent clouds. Cloud-top heights are not produced using GOES-10 Imager data because the 13.3 μm CO_2 channel is not available on this instrument. This product is expected to have the most utility in determining where airport visibility may be limited, either currently or in the future due to the advection of clouds and/or fog.

* *Corresponding author address*: Wayne F. Feltz, CIMSS/SSEC, 1225 West Dayton Street Room 238, Madison, WI, 53706; e-mail: wayne.feltz@ssec.wisc.edu.

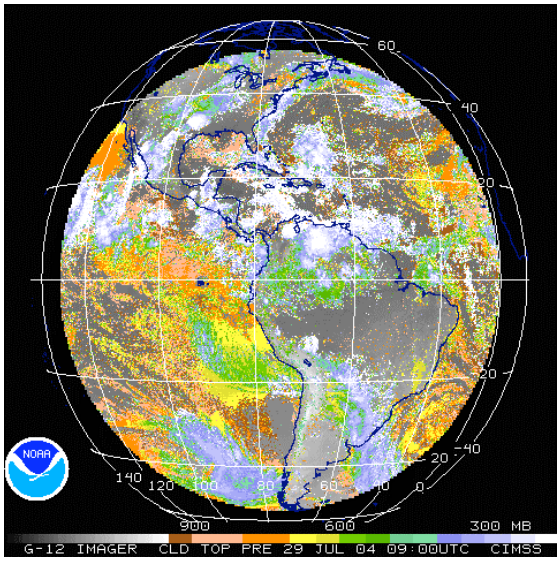

Figure 1: Sample image of cloud top pressure, derived using GOES-12 Imager data.

Validation studies have been performed using the ASAP CONUS cloud products. Specifically, the GOES-12 Imager and Sounder cloud top heights were compared to Cloud Physics Lidar (CPL) measurements from the Atlantic-THORPEX Regional Campaign (ATReC). This experiment was conducted in the winter of 2003 from Bangor, ME, and the CPL flew aboard the NASA ER-2 aircraft. Figure 2 shows the GOES-12 Imager (top- red) and GOES-12 Sounder (bottom-blue), as well as CPL (black) cloud-top heights from 05 Dec. 2003. The Imager heights show better agreement with the CPL than the Sounder heights due to the increased spatial resolution of the Imager. The best agreement for both satellite instruments is for mid-level clouds, while both the Sounder and Imager underestimate the CPL cloud-top height both for semi-transparent high clouds, and warm low-level clouds. Further validation for this product is an ongoing effort at CIMSS.

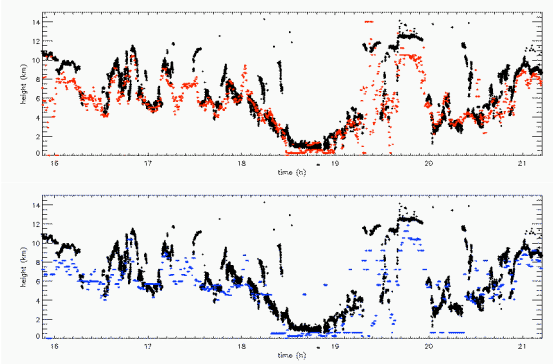

Figure 2: GOES-12 Imager (red) and Sounder (blue) cloud top height with CPL (black) cloud top height from the ATReC experiment.

In addition to the CONUS cloud products, cloud amount and cloud-top pressure are also available globally, and are derived using data from a suite of meteorological satellite instruments including GOES, MODIS, AVHRR, METEOSAT, and GMS. High temporal resolution geostationary data are used in the tropics and mid-latitudes, while the polar-orbiting AVHRR and MODIS are used to complete coverage over the polar regions. An example of the global cloud product cloud-top height is shown in Figure 3. This product uses a single wavelength (~11 μm) to determine cloud/no-cloud classifications globally. This technique is particularly useful for sensing clouds at high and mid-levels, however, sometimes miss low clouds and fog. Cloud top height is determined by comparing the ~11 μm brightness temperature (T_B) to a NWP model temperature profile. These data are expected to have the greatest utility over oceanic regions, where the lack of ground-based data is prohibitive to aviation forecasting.

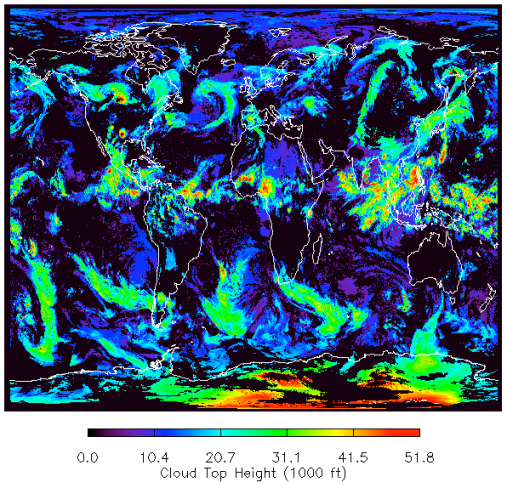

Figure 3: Sample image of cloud top height from the ASAP global cloud product.

3. CONVECTIVE PRODUCTS

Hazards related to thunderstorms (lightning, hail, strong winds and wind shear) cost the aviation industry many millions of dollars annually in lost time, fuel and efficiency through delayed, cancelled and rerouted flights, as well as accidents (Mecikalski et al. 2002; Murray 2002). Therefore, increased skill in forecasting thunderstorm initiation and evolution would be very beneficial to aviation interests.

Several products have been developed as part of the ASAP initiative to aid in the diagnosis and forecasting of convection-related aviation hazards. A classification algorithm has been developed to help identify several types of convectively-induced cloud features. This product is based upon a region growing (clustering) technique utilizing GOES visible (VIS) and multi-spectral IR data. GOES pixels are clustered based

upon statistical similarity. This classification system is produced at the 1 km GOES VIS resolution and currently identifies 5 types of convectively-induced clouds: 1) small, low-level cumulus, 2) mid-level cumulus, 3) mature cumulus clouds with depths extending through the entire troposphere, 4) thick anvil ice clouds, and 5) thin anvil and cirrus clouds. This product can be produced over both land and oceanic regions to identify potential locations of convectively-induced turbulence (CIT). This product also represents the foundation for a convective storm initiation (CI) nowcast product, for which only cumulus cloud pixels are processed, thereby reducing processing requirements and allowing for CI nowcasting over large geographical regions. An example of the convective cloud mask is shown in figure 4.

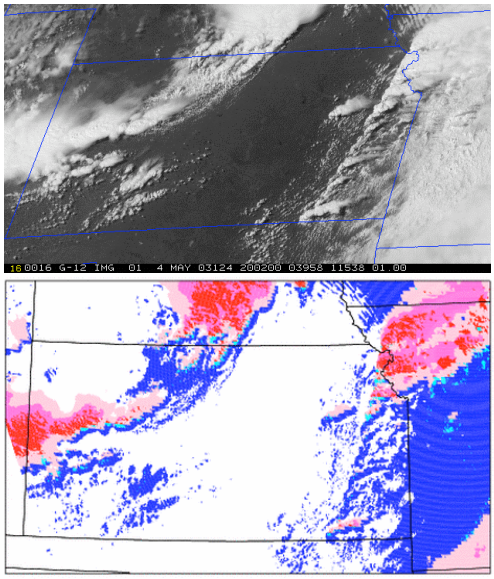

Figure 4: (top) 1 km resolution GOES-12 visible imagery at 2000 UTC on 4 May 2003. (bottom) The convective cloud classification, where blue is small low-level cumulus and thin water cloud, cyan is mid-level cumulus, red is mature cumulus, magenta is thick anvil ice cloud, and pink is thin anvil ice cloud.

Cloud-top trend estimates for moving cumulus represent the primary interest field within the ASAP CI nowcast algorithm. Roberts and Rutledge (2003, RR03 hereafter) show that the occurrence of sub-freezing 10.7 μm T_B's coupled with cooling rates of 8°C/15 mins provide up to 30 mins advance notice of CI (i.e. the first detection of 35 dBz reflectivity by WSR-88D). Cloud-top cooling trends are calculated here through the use of satellite–derived atmospheric motion vectors (AMVs) produced by the UW-CIMSS algorithm (Velden et al. 1997, 1998). Figure 5 shows an example of AMVs calculated from a 3-image sequence of GOES-12 data. The UW-CIMSS algorithm was adjusted for this research to capture flow from both the synoptic- and meso-scale. AMVs within the bottom panel are associated with immature cumulus, whereas AMVs in the middle and top panels are associated with developing cumulus and mature convection, respectively. A complete description of this technique can be found in Bedka and Mecikalski (2005).

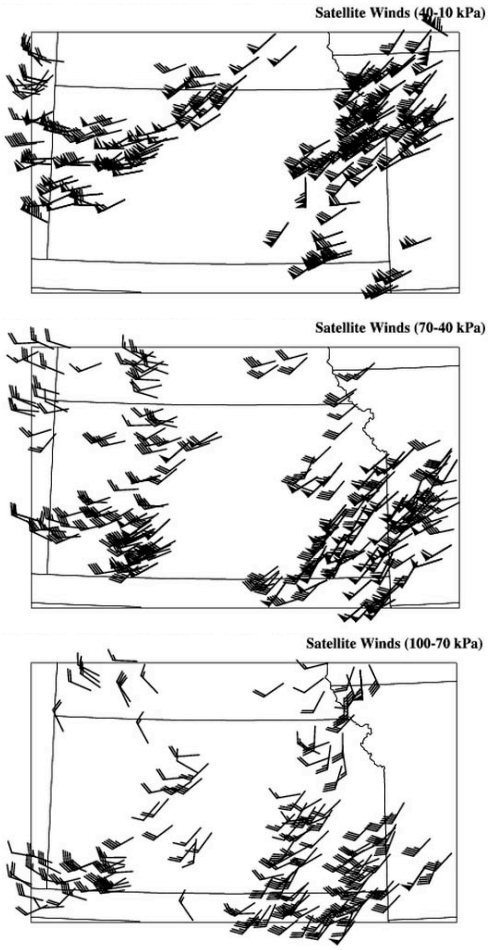

Figure 5: (top) The satellite-derived AMV field (in knots) within the 40-10 kPa layer. Only 20% of the winds are shown for clarity. (middle) Same as (top) but for the 70-40 kPa layer. (bottom) Same as (top) and (middle), but for the 100-70 kPa layer.

Through knowledge of the current AMV speed and direction, the past location of a cumulus cloud pixel can be found and cloud-top cooling rates can be determined. An example of these cloud-top cooling rates is shown in Figure 6 for developing convection occurring over northern Alabama. Figure 7 shows current and future (i.e. 30 mins later) radar reflectivity and lightning source counts over the same domain. As noted by RR03, locations of robust satellite-observed cloud growth correlate well with convective storm initiation and growth. Mecikalski and Bedka (2005) show that

cloud-top cooling rate information combined with other IR-based interest fields can provide a 30-60 min lead time in nowcasting convective initiation. The findings of these authors are further validated through comparison of these two figures, where locations of enhanced cloud-top cooling (>-20º C/30 mins) correspond well with future convective development. In addition, enhanced cloud-top cooling also appears to be related to an increase in cloud electrical activity. Cloud-top cooling is well correlated with cloud updraft width and strength (i.e. cumulus mass flux; M_c). Thus, we expect that locations of robust vertical cloud growth would be related to lightning occurrence, as M_c supplies the requisite amount of condensate necessary to drive electrical charge transfer and the development of electrical energy within a cloud. Future work will focus on quantifying optimal IR satellite-derived parameter values for lightning initiation nowcasting.

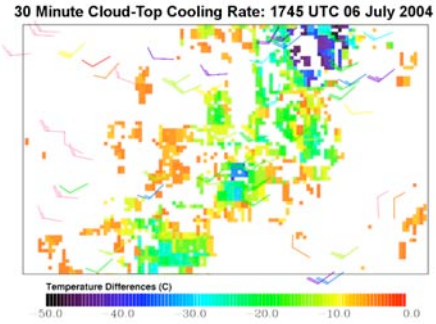

Figure 6: 30-min cloud-top cooling rates for moving cumulus clouds over northern Alabama at 1745 UTC on 6 July 2004. Also shown are satellite AMVs where warm (cool) colors correspond to lower- (upper-) tropospheric vectors.

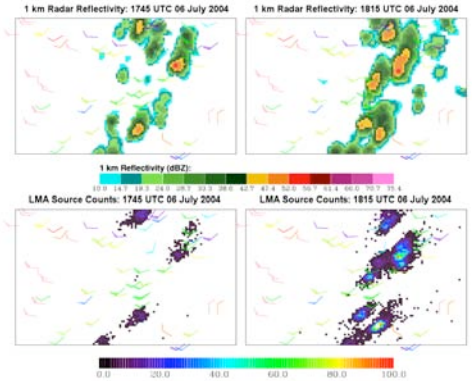

Figure 7: (top) WSR-88D reflectivity at a 1 km height, highlighting isolated developing convection at 1745 (left) and 1815 UTC (right) on 6 July 2004. (bottom) Northern Alabama Lightning Mapping Array (LMA) source count data showing an increase in cloud electrical activity over this 30 min period. Note the relationship between increased radar (lightning) reflectivity (activity) and cooling convective cloud tops shown in Figure 6.

4. SATELLITE TURBULENCE SIGNATURES

Turbulence presents a significant aviation hazard and can be caused by several sources. Convection, orography, and upper tropospheric instability on the synoptic-scale can all lead to significant turbulence episodes in both cloudy and "clear-air" conditions. Analysis of IR satellite data in spectral, temporal, and spatial domains is being conducted under the ASAP initiative to provide insight to the satellite identification of turbulent regions in the atmosphere. The approach is to provide the FAA Turbulence PDT's with fields of "interest" from pattern recognition and water vapor/ozone gradients.

Development of a GOES/MODIS satellite cloud and water vapor pattern recognition software for mountain-wave induced turbulence detection is in progress (Fig. 8). A combined effort using all satellite precursors will lead to a turbulence detection confidence mask. These ideas will be developed in collaboration with the Turbulence PDT. Other new methods for quantifying mountain-wave turbulence (i.e. trapped versus breaking mountain waves) in MODIS and GOES imagery, beyond simply identifying these features in imagery, are under development. Research will be toward making this product an interest field that may help isolate CIT or clear-air turbulence (CAT) over and downstream from thunderstorms and mountainous regions. A motivation of this satellite-based turbulence technique is the goal of identifying and characterizing regions of moderate and severe clear-air (e.g., mountain waves), and cloud induced turbulence (e.g., thunderstorms). An example of waves existing in MODIS water vapor imagery is shown in Fig. 8.

Another potential ASAP turbulence product would be to couple output from the convective cloud mask (Fig. 4), which can be developed for use with any satellite instrument data, with cloud-top cooling rate information to identify strong updrafts within cumulus clouds. A field of convective updraft location would be especially important for the Oceanic Weather PDT and Turbulence PDT.

An example of satellite-derived turbulence interest fields include a GOES water vapor gradient field that corrects for satellite viewing angle and temperature to provide an upper-tropospheric specific humidity product, which varies closely with tropopause height (Wimmers and Moody 2001; 2004a,b). As such, the more extreme gradients in the specific humidity imagery are closely correlated to areas tropopause folding, and an empirical model uses this relationship to predict regions of CAT-producing tropopause folds. Figure 9 shows an example of this empirical model, validated with contemporaneous pilot reports of turbulence. More information about this product can be found at: http://cimss.ssec.wisc.edu/asap/science.

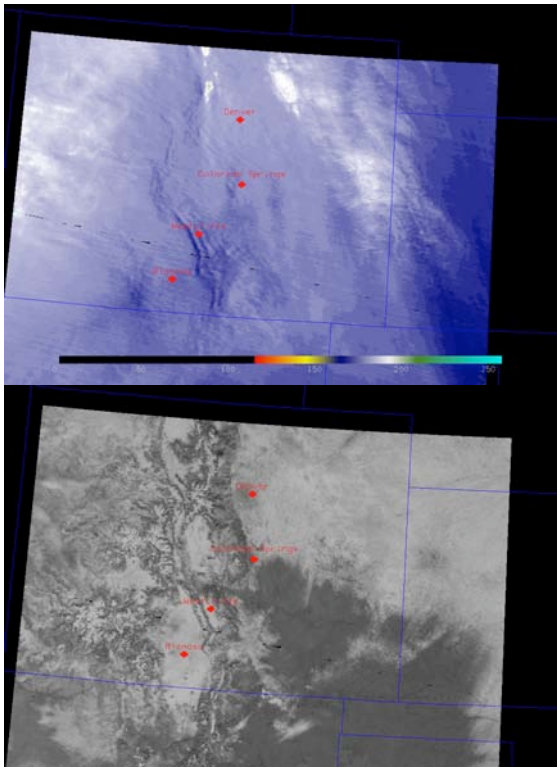

Figure 8: An example of mountain waves visible in the Terra MODIS water vapor imagery (6.7 um) but not "detected" in the visible imagery from 07 February 2004.

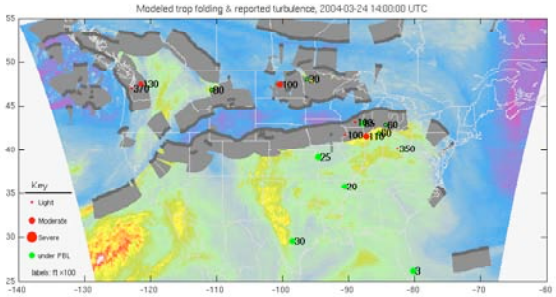

Figure 9: An example of possible regions of tropospheric folding determined through using a corrected GOES derived specific humidity field. Reports of aviation turbulence are plotted on the figure.

Another goal of this component of ASAP is to evaluate the utility of hyperspectral data (e.g., from the future GOES-R satellite) for detecting turbulence signatures. Future studies include using high vertical and spatial resolution numerical weather prediction model output containing turbulence to simulate observations by future hyperspectral resolution sensors. These studies will provide a preliminary indication of the ability of advanced high spectral resolution IR instrumentation (CrIS, IASI, HES, etc) to detect the presence of turbulence.

5. VOLCANIC ASH DETECTION

Volcanic ash has caused several nearly catastrophic commercial airline engine failures and windshield scoring incidents (Miller and Casadevall, 2000). Tracking the horizontal location and altitude of post-eruption ash plumes until the cloud disperses is critical to aviation safety and can have substantial economic impacts as well. Geostationary satellite (GEO) sounder and imager instrumentation offers relatively good temporal resolution for the monitoring of airborne ash resulting from volcanic eruptions. While GEO platforms provide better temporal resolution, their large fields of view and limited global coverage over volcanically active regions act as disadvantages for the tracking of volcanic ash in the atmosphere. In contrast, polar-orbiting satellite [low-Earth orbiting (LEO)] instruments such as the AVHRR and MODIS provide high spatial resolution and better global coverage but, in general, poor temporal sampling. However, at any given time there are several polar-orbiting satellites, each capable of detecting volcanic ash with fairly frequent time intervals at higher latitudes. This ongoing study focuses on determining how best to optimize current and future LEO and GEO satellite instrument capabilities in an effort to better monitor volcanic ash (both horizontal and vertical extent) in the atmosphere in an automated manner.

The methodology used in this research is based on the knowledge of spectral signatures resulting from the presence of suspended ash particles and high SO_2 gas concentrations. These spectral signatures are driven by the microphysical properties and by the indices of refraction of the volcanic aerosols. One such spectral signature, often termed the reverse absorption method (Prata, 1989), is characterized by negative 11 μm minus 12 μm brightness temperature differences. Most meteorological clouds have a positive 11 μm minus 12 μm brightness temperature difference. This standard technique will be referred to throughout this section.

Detection of SO_2 can also be useful in monitoring ash clouds when SO_2 is released along with ash during a volcanic eruption. While both SO_2 and ash do not always follow the same post-eruption trajectories (Seftor et al. 1997), monitoring SO_2 clouds does provide insight for locating possible regions of volcanic ash. Currently, SO_2 absorption channels are available at high spatial resolution on the MODIS instrument and at very high spectral resolution on the AIRS instrument, both of which can be used to demonstrate SO_2 detection capabilities. In the future (~2013) the GOES-R Advanced Baseline Imager (ABI) and Hyperspectral Environmental Sounder (HES) will

have similar capabilities as the MODIS and AIRS instruments.

Recent work has been focused on two areas: 1). Improving upon current standard ash detection techniques such as the reverse absorption method. The main goal is to develop rigorous algorithms that can be applied globally to a variety of geostationary and polar-orbiting satellite imagers. 2). Evaluating current cloud top height retrieval algorithms for use on volcanic plumes. The primary focus is on using satellite imagers since they currently offer much better spatial resolution than sounding instruments. Figure 10 shows the results of a new and improved ash detection algorithm (middle panel) compared to the standard reverse absorption method (bottom panel). The new method, which supplements the reverse absorption technique with visible and near-infrared channel data, results in a significant improvement in ash detection. This new method is also able to identify ice clouds that are heavily contaminated with volcanic aerosols, even though these clouds generally lack a reverse absorption signature. Although MODIS data were used in this example, the new ash detection algorithm utilizes channels that are common to almost all current and future imagers, so this technique could have been applied to just about any other imager. Also, in order to maximize future ash detection capabilities, more advanced techniques that take full advantage of the higher spectral resolution offered by future imagers such as the GOES-R Advanced Baseline Imager and the Visible/Infrared Imager/Radiometer Suite (VIIRS) are also being developed using MODIS as the prototype.

Two cloud top height retrieval algorithms, the CO_2 slicing technique and a split window 1DVAR retrieval, are also currently being evaluated for applications to volcanic plumes. Although the CO_2 slicing method (Wylie and Menzel, 1989) should be more accurate than the split window method (Heidinger *et al.*, 2005) for mid and upper tropospheric plumes, many imagers do not (and will not) have CO_2 absorption channels, so the split window algorithm may be a useful substitute when CO_2 slicing is not an option and may be more effective for plumes that reside in the lower troposphere. It should be noted that both height retrieval algorithms produce results that are consistent with the operational advisory height estimates for the eruption shown in Figure 10. Further evaluation of each algorithm is ongoing.

The next generation geostationary IR weather instruments (ABI, GIFTS and HES) will have spectral coverage similar to or exceeding existing instruments on polar orbiting satellites. This investigation, therefore, provides an opportunity to lay the ground work for future "volcanic ash detection" algorithms.

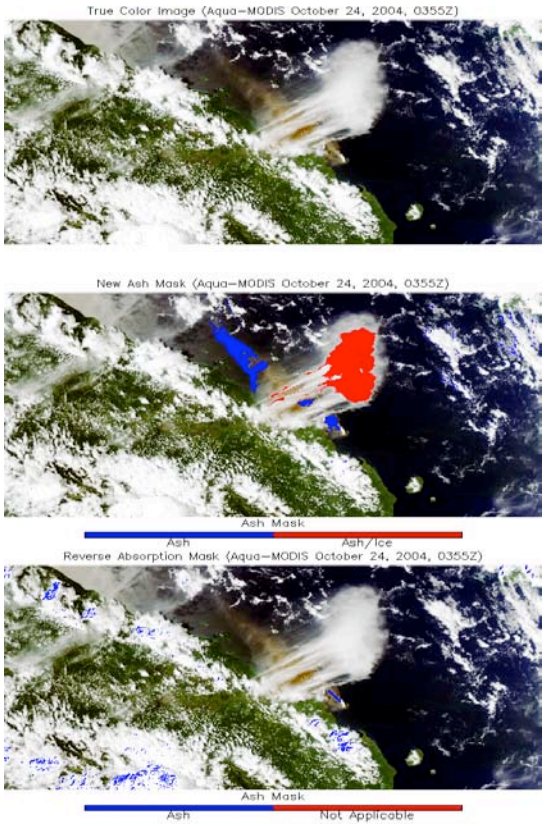

Figure 10: True color Aqua-MODIS images capturing an eruption of Manam, PNG on October 24, 2004, 0355 UTC. The top image is an unaltered true color image of the scene, the results of the new multispectral volcanic ash mask are overlaid on the middle image, and the ash mask given by identifying pixels with an 11 μm minus 12 μm brightness temperature difference less than 0.0 (reverse absorption technique) is shown in the bottom image. The new algorithm clearly improves upon the standard reverse absorption technique and also provides information on the location ice clouds that are contaminated with volcanic aerosols.

6. ACKNOWLEDGEMENTS

This research was supported by the NASA LaRC Subcontract #4400071484. More information can be found at http://cimss.ssec.wisc.edu/asap/

7. REFERENCES

Bedka, K. M. and J. R. Mecikalski, 2005: Applications of satellite-derived atmospheric motion vectors for estimating mesoscale flows. In Press. *J. Appl. Meteor.*

Heidinger, A. K., M. D. Goldberg, D. Tarpley, A. J. Jelenak, and M. J. Pavolonis, 2005: A new AVHRR cloud climatology. International Asia-Pacific Environmental Remote Sensing Symposium, 4th:

Remote Sensing of the Atmosphere, Ocean, Environment, and Space, Honolulu, Hawaii, 8-11 November 2004. Applications with Weather Satellites II (proceedings). Bellingham, WA, International Society for Optical Engineering, (SPIE), 197-205.

Mecikalski, J. R., D. B. Johnson, J. J. Murray, and many others at UW-CIMSS and NCAR, 2002: NASA Advanced Satellite Aviation-weather Products (ASAP) study report, NASA Technical Report, 65 pp. [Available from the Schwerdtferger Library, 1225 West Dayton Street, Univ. of Wisconsin-Madison, Madison, WI 53706.].

------, and K. M. Bedka, 2004: Forecasting convective initiation by monitoring the evolution of moving cumulus in daytime GOES imagery. In press. *Mon. Wea. Rev.*

Miller, T. P., and T. J. Casadevall, 2000: Volcanic ash hazards to aviation. *Encyclopedia of Volcanoes,* edited by H. Sigurdsson, pp. 915-930, Academic, San Diego, Calif.

Murray, J. J., 2002: Aviation weather applications of Earth Science Enterprise data. Earth Observing Magazine, 11, No. 8, (August 2002).

Prata, A. J., 1989: Observations of volcanic ash clouds in the 10 –12 micrometer window using AVHRR/2 data. *Int. J. Rem. Sen.*, **10**, 751-761

Roberts, R. D., and S. Rutledge, 2003: Nowcasting storm initiation and growth using GOES-8 and WSR-88D data. *Wea. Forecasting*, **18**, 562-584.

Schreiner, A. J., T. J. Schmit, and W.P Menzel, 2001: Observations and trends of clouds based on GOES sounder data. *J. Geophys. Res.*, **106,** 20,349-20,363.

Seftor, C. J., N. C. Hsu, J. R. Herman, P. K. Bhartia, O. Torres, W. I. Rose, D. J. Schneider and N. Krotkov, 1997: Detection of volcanic ash clouds from Nimbus-7/TOMS, *J. Geophys. Res., 102: 16749-16760.*

Velden, C. S, C. M. Hayden, S. J. Nieman, W. P. Menzel, S. Wanzong, J. S. Goerss, 1997: Upper-tropospheric winds derived from geostationary satellite water vapor observations. *Bull. Amer. Meteor. Soc.*, **78**, 173-195.

------, T. L. Olander, and S. Wanzong, 1998: The impact of multispectral GOES-8 wind information on Atlantic tropical cyclone track forecasts in 1995. Part I: Dataset methodology, description, and case analysis. *Mon. Wea. Rev.*, **126**, 1202-1218.

Wimmers, A. J., and J. L. Moody 2001: A fixed-layer estimation of upper tropospheric specific humidity from the GOES water vapor channel: Parameterization and validation of the altered brightness temperature product, J. Geophys. Res., 106 (D15), 17115-17132.

------, and J. L. Moody, 2004: Tropopause folding at satellite-observed spatial gradients, I. Verification of an empirical relationship, J. Geophys. Res., in print.

------, and J. L. Moody, 2004: Tropopause folding at satellite-observed spatial gradients, II. Development of an empirical model, J. Geophys. Res., in print.

Wylie, D. P., and W. P. Menzel, 1989: Two years of cloud cover statistics using VAS. *J. Climate,* **2,** 380-392.